

Electronic Supplementary Information

Construction of a self-directed replication system for label-free and real-time sensing repair glycosylases with zero background

Li-juan Wang[†], Ying-ying Lu[†], and Chun-yang Zhang*

College of Chemistry, Chemical Engineering and Materials Science, Collaborative Innovation Center of Functionalized Probes for Chemical Imaging in Universities of Shandong, Key Laboratory of Molecular and Nano Probes, Ministry of Education, Shandong Provincial Key Laboratory of Clean Production of Fine Chemicals, Shandong Normal University, Jinan 250014, China.

* Corresponding author. Tel.: +86 0531-86186033; Fax: +86 0531-82615258. E-mail: cyzhang@sdu.edu.cn.

1. Schematic illustration of the recycling amplification (I) in Scheme 1B.

As illustrated in Fig. S1, after the formation of a one-stem-loop DNA (I) with B2c in the loop, BIP can hybridize with the loop of one-stem-loop DNA (I) to successively initiate the SDS and the self-primed polymerization extension, generating a long one-stem-loop DNA (I-I) which contains a loop with B2c and simultaneously releasing a long double-stem-loop DNA (I-I) which contains B2 and B2c in the loops, respectively. The newly generated one-stem-loop DNA (I-I) can be further hybridized by BIP to continuously initiate new rounds of SDS and the self-primed polymerization extension, yielding abundant stem-loop DNAs and dsDNA intermediates with much longer length (i.e., the recycling amplification I-I). Meanwhile, the newly released longer double-stem-loop DNA (I-I) can induce the self-primed polymerization extension to form a one-stem-loop DNA with B2c in the loop. BIP will then hybridize with the loop to prime the SDS to produce a dsDNA intermediate containing one loop with B2c, which can further initiate the self-primed polymerization extension and the SDS to generate a new one-stem-loop DNA (I-I) and simultaneously release a new double-stem-loop DNA (I-I). The newly produced one-stem-loop DNA (I-I) and double-stem-loop DNA (I-I) can start new rounds of amplification reaction described as above. With the proceeding of reactions, large amounts of the mixtures of stem-loop DNAs and dsDNA intermediates with various lengths will be generated in the recycling amplification (I). At same time, FIP can hybridize with the loop of one-stem-loop DNA (II) to initiate the recycling amplification (II), generating large amounts of stem-loop DNAs and dsDNA intermediates same to those obtained in recycling amplification (I). As a result, large amounts of the amplification products with different length are produced during the self-directed exponential replication process.

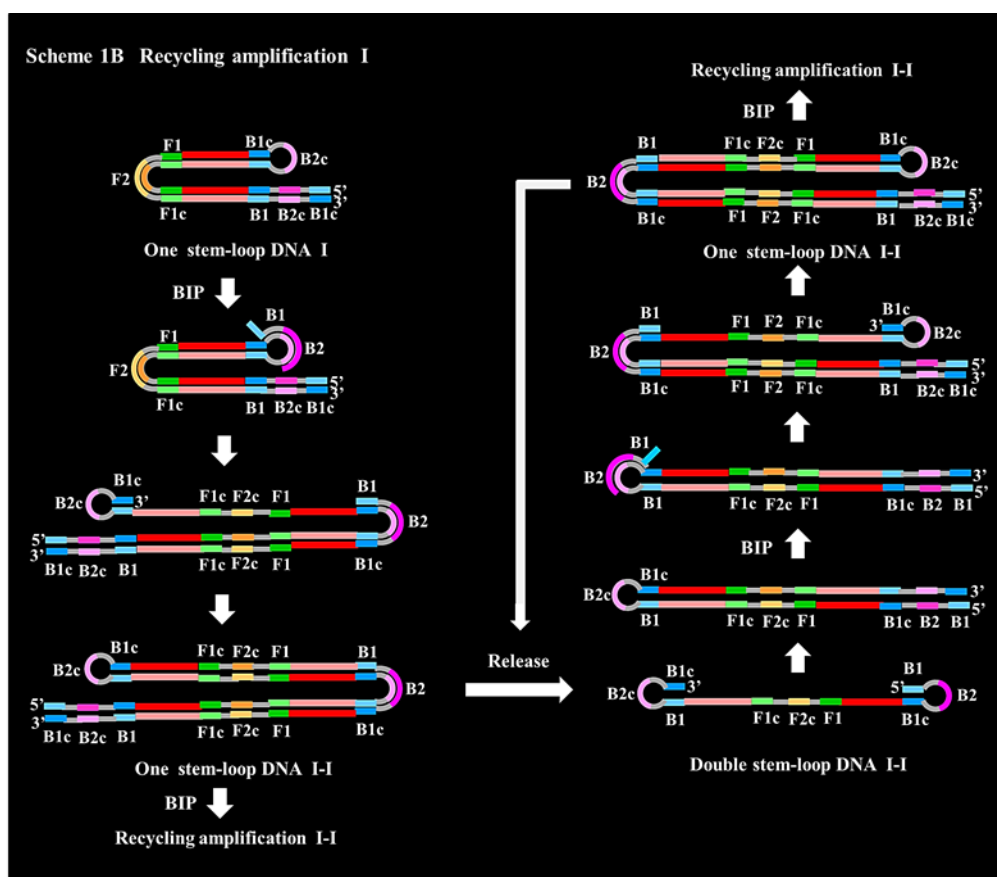


Fig. S1 Schematic illustration of the recycling amplification (I) in Scheme 1B.

2. Optimization of the amount of *Bst* DNA polymerase.

The DNA repairing-driven self-directed exponential replication reaction is dependent on the autocycling polymerization extension and strand-displacement DNA synthesis (SDS) catalyzed by *Bst* DNA polymerase, and thus the amount of *Bst* DNA polymerase is an important parameter and should be optimized. When the amount of *Bst* DNA polymerase increases from 1 to 6 U, the amplification reaction is correspondingly accelerated (Fig. S2A), resulting in the decrease of POI values (Fig. S2B). When the amount of *Bst* DNA polymerase is more than 6 U, the amplification reaction begins to slow down, leading to the gradual increase of POI values (Figs. S2A-2B). Therefore, 6 U of *Bst* DNA polymerase is used in the subsequent research.

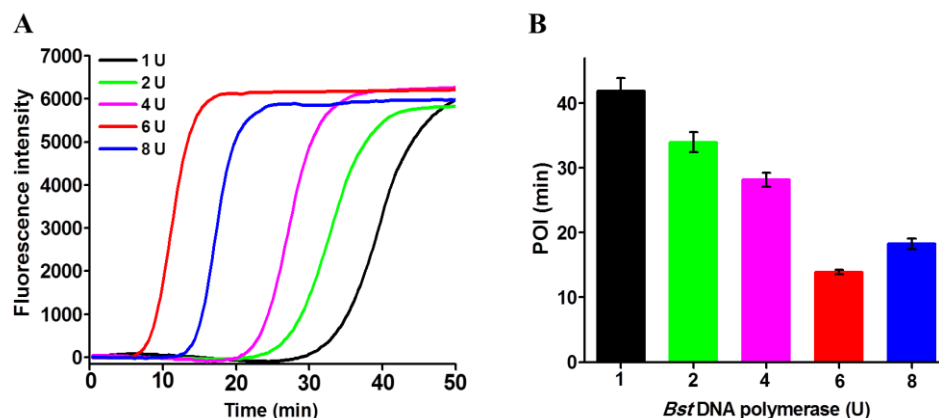


Fig. S2 (A) Real-time fluorescence curves in response to different amounts of *Bst* DNA polymerase in the range from 1 to 8 U. (B) Measurement of POI values of the real-time fluorescence curves in A. The error bars represent standard deviations of three independent experiments.

3. Optimization of the ratios of both FIP to FOP and BIP to BOP.

The forward primers FIP and FOP can hybridize with the unfolded stem-loop DNA template to initiate the polymerization extension and SDS, producing the starting materials (i.e., the double-stem-loop DNA) for self-directed exponential replication with the assistance of backward primers BIP and BOP. Moreover, the implementation of subsequent self-directed exponential replication is mediated by forward primer FIP and backward primer BIP. Thus, the ratio of FIP to FOP is an important parameter and should be optimized. As shown in Fig. S3A, the amplification efficiency enhances with the increasing FIP to FOP ratio from 1:1 to 4:1, and begins to slow down beyond the ration of 4:1, resulting in the decrease of POI value from 1:1 to 4:1 and the increase of POI value from 4:1 to 8:1 (Fig. S3B), respectively. This can be explained by two factors: (1) at low FIP-to-FOP ratio, the relatively high amount of primer FOP may disturb the hybridization of primer FIP with the unfolded DNA template, adversely affecting the subsequent polymerization

extension and SDS; (2) at high FIP-to-FOP ratio, the low amount of primer FOP may limit the amplification reaction, adversely influencing the efficiency of self-directed exponential replication reaction. Thus, the optimal FIP-to-FOP ratio of 4:1 is used in subsequent research.

Backward primers BIP and BOP also participate in the formation of starting materials (i.e., the double-stem-loop DNA), and backward primer BIP further mediates the performing of self-directed exponential replication. Thus, the ratio of BIP to BOP is a critical parameter and should be optimized. As shown in Fig. S4, when the ratio of BIP to BOP increases from 1:1 to 8:1, the amplification efficiency enhances from 1:1 to 4:1, and gradually decreases from 4:1 to 8:1 (Fig. S4A), accompanied by the reduction of POI value from 1:1 to 4:1 and the increase of POI value from 4:1 to 8:1 (Fig. S4B), respectively. Therefore, the BIP-to-BOP ratio of 4:1 is used in subsequent research.

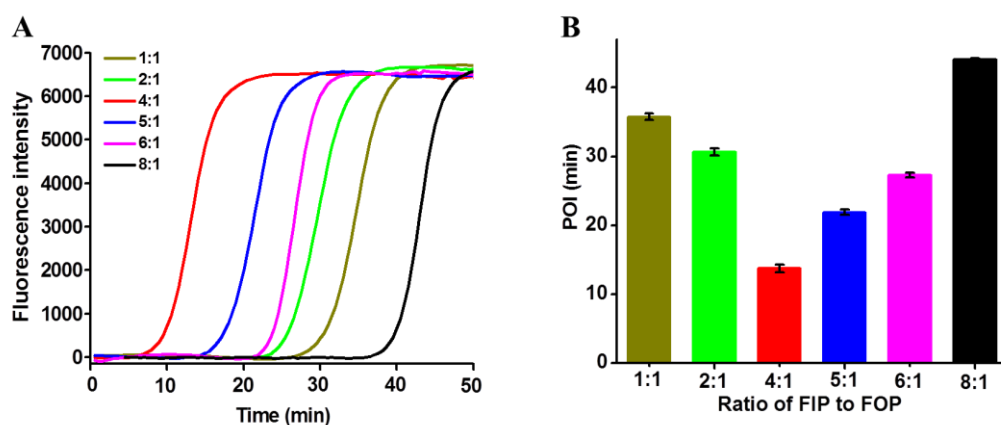


Fig. S3 (A) Real-time fluorescence curves in response to different ratio of FIP to FOP in the range from 1:1 to 8:1. (B) Measurement of POI values of the real-time fluorescence curves in A. The error bars represent standard deviations of three independent experiments.

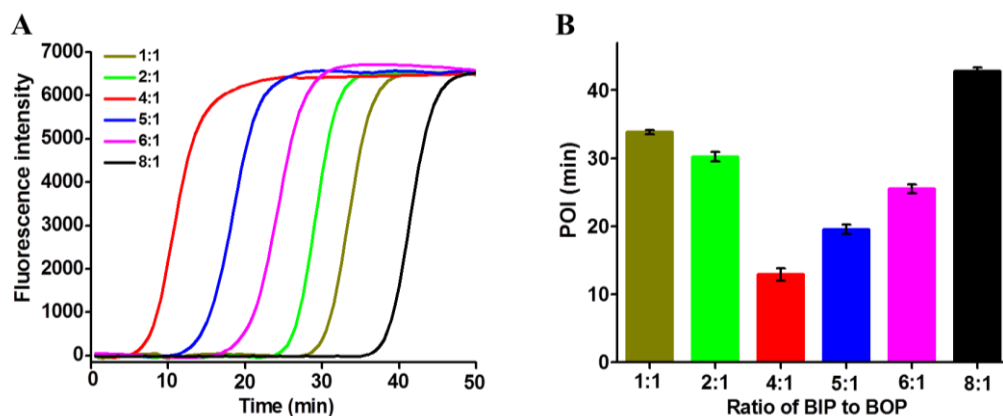


Fig. S4 (A) Real-time fluorescence curves in response to different ratio of BIP to BOP in the range from 1:1 to 8:1. (B) Measurement of POI values of the real-time fluorescence curves in A. The error bars represent standard deviations of three independent experiments.

4. Effect of CdCl₂ upon Bst DNA polymerase activity.

To investigate the effect of CdCl₂ upon the activity of Bst DNA polymerase, we have to eliminate the interference of repair glycosylase hOGG1. A synthetic 132 nt sequence that corresponds to the longer excision product of hOGG1 is used as the unfolded DNA template to carry out the self-directed exponential replication reaction. As shown in Fig. S5, the well-defined real-time fluorescence signal in a sigmoidal fashion is observed in the presence of CdCl₂ (Fig. S5A, red curve), which is comparable to that obtained in the absence of CdCl₂ (Fig. S5A, black curve). Moreover, the corresponding POI value in the presence of CdCl₂ (Fig. S5B, red column) shows no significant change compared with that in the absence of CdCl₂ (Fig. S5B, black column). These results demonstrate that CdCl₂ has no significant effect on the activity of Bst DNA polymerase, and thus it will not interfere with any process of the proposed method.

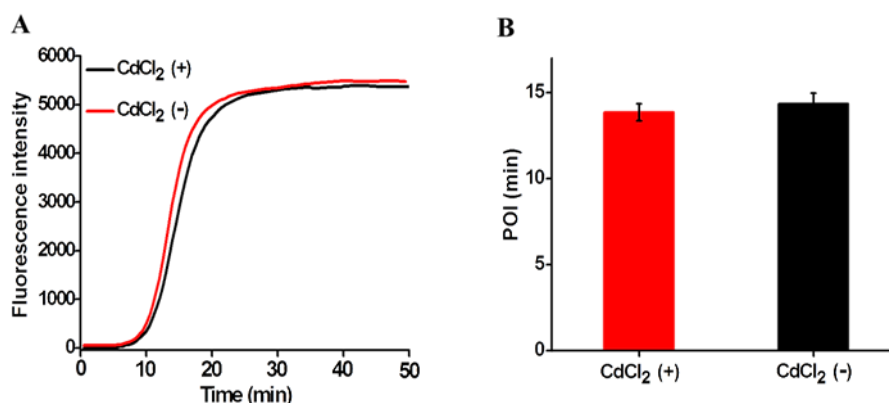


Fig. S5 (A) Real-time fluorescence curves in the presence and absence of 100 μ M CdCl₂, respectively. (B) Measurement of POI values of the real-time fluorescence curves in A. The concentration of the synthesized excision product (132 nt) is 450 nM. The error bars represent standard deviations of three independent experiments.

5. Cellular hAAG analysis with western blotting.

To evaluate the expression level of hOGG1 enzyme in different cancer cells, we used western blotting (Fig. S6) to analyze the protein extracts from the nucleus. As shown in Fig. S6A, we investigated the level of hOGG1 enzyme from A549 cells, HeLa cells, and MCF-7 cells using the rabbit anti-hOGG1 polyclonal antibody. Distinct bands (~39 KDa) are observed in response to A549 cells (Fig. S6A, lane 1), HeLa cells (Fig. S6A, lane 2), and MCF-7 cells (Fig. S6A, lane 3), respectively. Moreover, the intensities of above bands are semi-quantified by densitometry. With the internal reference protein (i.e., actin) as the control, the relative intensities in response to A549 cells (Fig. S6B, green column), HeLa cells (Fig. S6B, red column) and MCF-7 cells (Fig. S6B, blue column) can be obtained. Fig. S6B shows that the hOGG1 enzyme is highly expressed in A549 cells, HeLa cells, and MCF-7 cells, consistent with the previous reports.¹⁻³

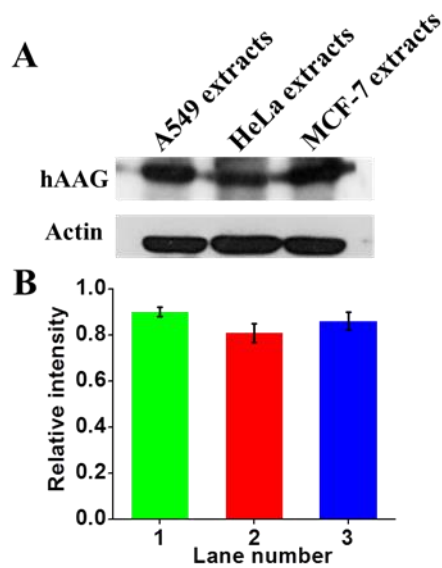


Fig. S6 (A) Analysis of hOGG1 expression in A549 cells (lane 1), HeLa cells (lane 2), and MCF-7 cells (lane 3), respectively. (B) Relative intensities of bands in response to A549 cells (green column), HeLa cells (red column), and MCF-7 cells (blue column), respectively. The relative intensity is the ratio value of I_t / I_i (I_t is the band intensity in response to target sample (i.e., A549 cells, HeLa cells, and MCF-7 cells), and I_i is the band intensity in response to the internal reference protein (i.e., actin)). Error bars represent the standard deviations of three experiments.

Table S1. Sequences of the oligonucleotides ^a

note	sequences (5'-3')
DNA template	ACT TTA TGC TTC TGT TGT GTG GAA TTG TGA ACA ATT TCA GTA CCC GGG GAT CCT CTA <i>CCT GCA GGC ATG CAA GCC</i> AAC GTC GTG ACT GGG AGG CGT TAC CCG TAA TAG CGA AGA GGC CAA CTA TAC <i>AAC CGC <u>QTG</u> CAT GCC TGC AGG T-P</i>
excision product	ACT TTA TGC TTC TGT TGT GTG GAA TTG TGA ACA ATT TCA GTA CCC GGG GAT CCT CTA CCT GCA GGC ATG CAA GCC AAC GTC GTG ACT GGG AGG CGT TAC CCG TAA TAG CGA AGA GGC CAA CTA TAC AAC CGC
forward inner primer	ACA ACG TCG TGA CTG GGA AAA CCC TTT TTG GCC TCT TCG CTA TTA C
backward inner primer	CGA CTC TAG AGG ATC CCC GGG TAC TTT TTG TTG TGT GGA ATT GTG
forward outer primer	TAG TAG GTT GTA TAG TT
backward outer primer	TCG TAA CTT TAT GCT TC

^a In DNA template, the italicized regions symbolize the complementary sequences, the underlined letter “O” symbolizes the oxidized guanine (8-oxoG), and the letter “P” at the 3’ end symbolizes the modified phosphate group.

Table S2. Sequences of the specific DNA templates for DNA repair enzymes ^a

note		sequences (5'-3')
DNA template	hOGG1	ACT TTA TGC TTC TGT TGT GTG GAA TTG TGA ACA ATT TCA GTA CCC GGG GAT CCT CTA CCT GCA GGC ATG CA <u>A</u> GCC AAC GTC GTG ACT GGG AGG CGT TAC CCG TAA TAG CGA AGA GGC CAA CTA TAC AAC CGC <u>O</u> TG CAT GCC TGC AGG T-P
	AAG	ACT TTA TGC TTC TGT TGT GTG GAA TTG TGA ACA ATT TCA GTA CCC GGG GAT CCT CTA CCT GCA GGC ATG CA <u>T</u> GCC AAC GTC GTG ACT GGG AGG CGT TAC CCG TAA TAG CGA AGA GGC CAA CTA TAC AAC CGC <u>I</u> TG CAT GCC TGC AGG T-P
	UDG	ACT TTA TGC TTC TGT TGT GTG GAA TTG TGA ACA ATT TCA GTA CCC GGG GAT CCT CTA CCT GCA GGC ATG CA <u>A</u> GCC AAC GTC GTG ACT GGG AGG CGT TAC CCG TAA TAG CGA AGA GGC CAA CTA TAC AAC CGC <u>U</u> TG CAT GCC TGC AGG T-P
	TDG	ACT TTA TGC TTC TGT TGT GTG GAA TTG TGA ACA ATT TCA GTA CCC GGG GAT CCT CTA CCT GCA GGC ATG CA <u>G</u> GCC AAC GTC GTG ACT GGG AGG CGT TAC CCG TAA TAG CGA AGA GGC CAA CTA TAC AAC CGC <u>T</u> TG CAT GCC TGC AGG T-P

^a In DNA template of hOGG1, the underlined letters “O” and “A” symbolize the oxidized guanine (8-oxoG) and its matched base, respectively. In DNA template of AAG, the underlined letters “O” and “A” are substituted for the letters “I” and “T”, respectively, and the letter “I” symbolizes the oxidized 2'-deoxyinosine. In DNA template of UDG, the underlined letters “O” and “A” are

substituted for the letters “U” and “A”, respectively, and the letter “U” symbolizes the uracil. In DNA template of TDG, the underlined letters “O” and “A” are substituted for the letters “T” and “G”, respectively, and the letter “T” symbolizes the thymine.

References

1. Y. Zhang, C.-c. Li, B. Tang, and C.-y. Zhang, *Anal. Chem.*, 2017, **89**, 7684-7692.
2. L.-j. Wang, F. Ma, B. Tang, and C.-y. Zhang, *Anal. Chem.*, 2016, **88**, 7523-7529.
3. E. Gollapalle, R. Wang, R. Adetolu, D. Tsao, D. Francisco, G. Sigounas, A. G. Georgakilas, *Radiat. Res.*, 2007, **167**, 207-216.